# Modelling Diffusion-Weighted Steady-State Free Precession in Terms of the Reciprocal Spatial Wave Vector and Non-Gaussian Diffusion Probability Density Functions

**J. A. McNab[1], and K. L. Miller[1]**

[1]Oxford Centre for Functional Magnetic Resonance Imaging of the Brain, University of Oxford, Oxford, United Kingdom

**Introduction** Diffusion-weighted steady-state free precession (DW-SSFP) accumulates signal from multiple echoes over several TRs yielding a strong sensitivity to diffusion with short gradient durations and imaging times. DW-SSFP is thus of great interest as a potential method for high angular and spatial resolution diffusion imaging. The DW-SSFP signal is well characterized for isotropic, Gaussian diffusion[1-3], however, it is unclear how the multi-echo DW-SSFP signal propagates in inhomogenous media such as brain tissue. Previously we have explored DW-SSFP behaviour under conditions of anisotropic diffusion using a single diffusion tensor[4-5]. It has long been recognized, however, that the single tensor model can be inappropriate when crossing fibres, restrictive boundaries and/or semi-permeable membranes, are found within a single voxel. For this reason, model-free **q**-space methods[6] are becoming the preferred method to study the translational displacement distribution of water molecules within white matter. In this study, the DW-SSFP signal equation is presented for the first time in terms of the reciprocal spatial wave vector (**q**) and an arbitrary diffusion probability density function *pdf* (P(**r**,Δ)). The unique relationship between **q** and the DW-SSFP signal is investigated and the general form of the signal equation is validated through Monte Carlo simulations of individual spins.

**Theory** Assuming ($\delta << \Delta$)[6] and following Buxton's approximate partition analysis[3] which assumes that signal does not survive the transverse plane for more than two TR intervals, the signal (*S*) for a single echo pathway contributing to the total DW-SSFP signal in terms of an arbitrary diffusion *pdf* can be written,

$$S(n) = K * M(n) * \int P(\mathbf{r},\Delta=(n+1)*TR)\exp(-i2\pi\mathbf{q}\bullet\mathbf{r})d\mathbf{r} \quad \text{with} \quad K = \frac{-M_0(1-E_1)E_1E_2^2\sin\alpha}{(2-2E_1\cos\alpha)} \quad \text{and} \quad M(n) = \begin{cases}(1-\cos\alpha), & for\ n\ = 0\\ \sin^2\alpha*(E_1\cos\alpha)^{n-1}, & for\ n > 0\end{cases} \qquad (1)$$

where *n* is the number of longitudinal periods between the two transverse periods that form the echo. $M_0$ is the equilibrium magnetization, $\alpha$ is the flip angle, $E_1 = \exp(-TR/T_1)$, $E_2 = \exp(-TR/T_2)$ and P(**r**, Δ = *(n+1)*TR*) is the diffusion *pdf* which describes the probability of a particle traveling a distance **r** in time Δ = *(n+1)*TR*. The measured DW-SSFP is thus equal to the summation of Eq. 1 from n = 0 to ∞. In contrast to the elegant Fourier transform (FT) relationship which exists between **q** and the DW-SE signal attenuation, for DW-SSFP the signal is given by a summation of many FTs where each FT represents a different contributing echo pathway with a different diffusion time (Δ = (n+1)*TR). To demonstrate the implications of this dependence we examine two non-Gaussian systems. The first example is two tensors ($\mathbf{D}_1$ and $\mathbf{D}_2$) at different orientations with relative fractions *f* and (1-*f*). The second example is reflective boundaries, separated by a distance, *a*, for which the *pdf* and FT of the *pdf* has been presented previously by Tanner and Stejskal[7].

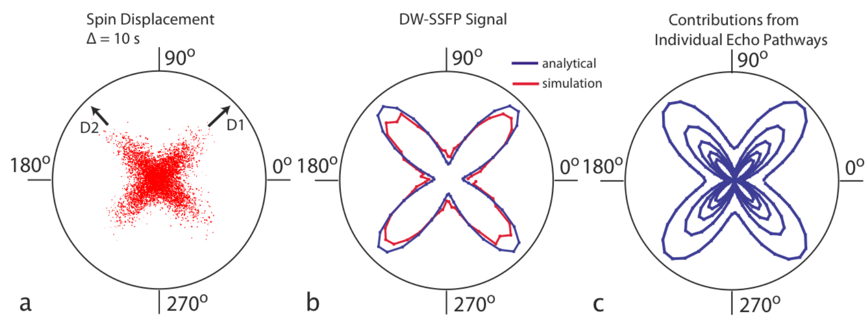


**Figure 1**: a) The spin displacement (Δ =10 s) of 10 000 spins commencing at (0,0) and diffusing according to Eq. 2 which describes two equivalent tensors (D1, D2) oriented at 45° and 135°, each having $\lambda_1/\lambda_2 = 1\times10^{-3}/1\times10^{-4}$. Spins were divided equally between the two tensors ( i.e. *f* = 0.5). b) DW-SSFP signal profiles derived from the summation of Eq.1 over n = 1 to n = 5 (blue) and the summation of individual protons magnetization evolutions after a period of 10s (red). c) Profiles of the DW-SSFP signal contributions from five different echo pathways (Eq. 1 with n = 1 - 5). The echo pathway with the longest diffusion time (n = 5) is at the centre and extending outwards are echo pathways with decreasing diffusion times.

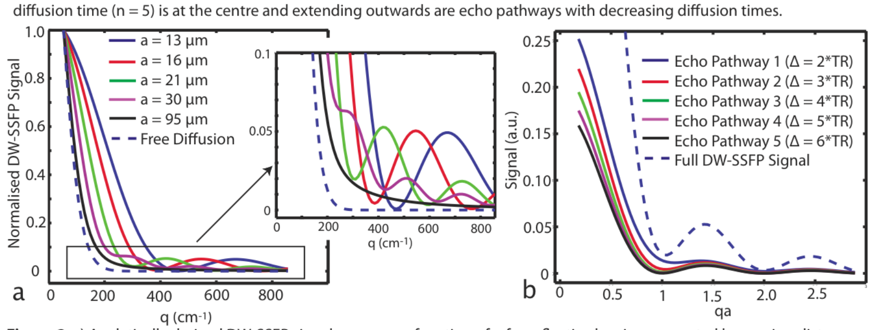


**Figure 2**: a) Analytically derived DW-SSFP signal curves as a function of q for reflective barriers separated by varying distances *a*. b) Signal contributions of individudal echo pathways which each have their own diffusion time (Δ) and the full DW-SSFP signal (i.e. the weighted combination of all five echo pathway signals) as a function of (q*a) for a = 21μm.

**Methods** DW-SSFP signal profiles were simulated in 2D by substituting the *pdf* corresponding to two orthogonal tensors into Eq. 1. To further verify the general form of the DW-SSFP signal equation (Eq. 1) Monte Carlo methods were used to simulate the stochastic motion and magnetization evolution of individual protons. The 2D diffusion of 10 000 protons were simulated with Δt = 50 μs time steps for a period of 10 s. The resultant displacements of two identical tensors ($\lambda_1/\lambda_2 = 1\times10^{-3}/1\times10^{-4}$ mm²/s), oriented orthogonal to each other at 45° and 135° were simulated with equal fractions (*f* = 0.5). Diffusing spins in each fibre population were simulated with a series of random displacements ($l_D$) generated from a Gaussian distribution with mean $< l_D> = 0$, standard deviation $\sigma_{lD} = (2\lambda_1\Delta t)^{1/2}$ and $\sigma_{lD} = (2\lambda_2\Delta t)^{1/2}$ along the principal and secondary diffusion axis respectively. RF pulse rotation, $T_1/T_2$ relaxation and diffusion gradient dephasing matrices were applied to each of the protons for consecutive TRs using α = 30°, TE/TR/$T_1$/$T_2$ = 5/45/700/90 ms and a diffusion gradient with amplitude 4 G/cm and duration 20 ms. Simulations were repeated for 30 diffusion directions (Δθ = 6°). The simulation commenced with all spins at (0,0) and total magnetization [$M_x$ $M_y$ $M_z$] = [0 0 1]. The diffusion gradient was assumed to be the only source of dephasing within each TR. At the end of the simulation the DW-SSFP signal was calculated from the summation of all of the proton's individual magnetizations. The effect of restriction on the DW-SSFP signal was also investigated using Eq. 1 with the *pdf* for spins trapped between perfectly reflecting rectangular barriers[7] and the same parameters as used for the crossing fibre example.

**Results and Discussion** Figure 1a shows the spin displacement profile at t = 10 s for 10 000 spins, diffusing according to Eq. 2. Figure 2b plots the resultant DW-SSFP signal profile for the diffusion *pdf* modeled in Fig. 1a. The analytical solution (Fig. 1b, blue line) is in good agreement with the Monte Carlo simulations (red line). In Figure 1c, the DW-SSFP signal profiles of the five echo pathways (Eq. 1, n = 1 to 5) are plotted. The weighted summation of these signals provides the analytical solution presented in Fig. 1b. Each echo pathway that contributes to the measured DW-SSFP signal represents a snapshot of the diffusion *pdf* at a different point in time. This is a very different behaviour from that exhibited in DW-SE where the signal is completely described by a single *pdf* with a well-defined diffusion time. A single *pdf* is insufficient by itself to explain the signal observed in Fig. 1b. In this sense, DW-SSFP is sensitive to the "process" of diffusion in a way that other diffusion pulse sequences are not. As a consequence, it is not straightforward to infer directly on a diffusion *pdf* given a DW-SSFP sampling of **q**-space. Despite this, Figure 2 demonstrates that the DW-SSFP signal is still sensitive to effects of restriction. Signal curves as a function of **q** show well-defined inflection points for specific restriction lengths (Fig. 2a). Based on the parameters used in Figure 2, it appears that DW-SSFP is sensitive to restriction on length-scales of 30 μm or less which is well within the regime of axon diameters and other types of cytoarchitecture.

**Acknowledgments and References** Funding provided by the Charles Wolfson Charitable Trust. (1) Kaiser R. J. Chem. Phys. 60:2966-79 (1974). (2) Wu E.X. JMR 90:243-253 (1990). (3) Buxton R. MRM 29:235-43 (1993). (4) McNab J.A. ISMRM 2006 (5) McNab J.A. ISMRM 2007 (6) Callaghan P.T. Principles of NMR Microscopy, OUP, 1991. (7) Tanner J.E. Chem. Phys. 49:1768 (1968).